Chofore et al. Int J Concr Struct Mater (2022) 16:70
https://doi.org/10.1186/s40069-022-00560-6

International Journal of Concrete Structures and Materials

RESEARCH

Open Access

Experimental Investigation on Bond, Microstructure and Durability of Expired Hardened Cement Blended with Ground Granulated Blast Furnace Slag as Partial Replacement of Cement in High-Strength Concrete

Ashenafi Tofu Chofore[1*], Bahiru Bewket Mitikie[2] and Abenezer Tariku Haile[3]

Abstract

The current study aimed to investigate the influence of the expired hardened cement blended with ground granulated blast furnace slag on the bond, microstructure, and durability of high-strength concrete (HSC). Five concrete mixes are prepared; the first mix is taken as a control, and the remaining four mixes are used as experimental blends. HSC characteristics are evaluated by compressive, flexural, splitting tensile, bond, and durability tests. Furthermore, the ultrasonic pulse velocity and microstructural characteristics tests are carried out to check concrete quality. The synergistic action of blends (expired harden cement with GGBS) on the strength test results was found to increase with an increase in blends up to 20%. The durability result reveals that HSC was found to be impermeable under aggressive conditions. The microstructural characteristics achieved in the current investigation explain the above strength, bond, and durability performance of these mixes. The whole performance of blends in HSC is adequate for industrial use.

Keywords: Expired hardened cement, Partial replacement, Cement, GGBS

1 Introduction

Nowadays, construction has become the most vital component in developing our planet and our country, and it plays a critical role in the social economy, especially in decreasing unemployment. On the other hand, as the population grows and improves its lifestyle, a proportional increase in the consumption of natural resources and energy occurs. Furthermore, the quick growth of the construction industry (CI) has advanced to a high consumption of material resources. Conversely, due to poor management techniques, the waste (construction and demolition waste) generated by the construction industry and its disposal in developing nations is considerable. These waste products are deposited directly into the environment as landfills, which can pollute the ecosystem. When we talk about the issue of construction, it is directly or indirectly related to the production of concrete (Andal et al., 2016; Bao et al., 2018; Gashahun, 2020; Saidi et al., 2014; Soares et al., 2014).

Besides, related to CO_2, global building materials production stands as the world's third-largest industrial sector, the extreme of which is related to the production of concrete. Moreover, concrete production is responsible

Journal information: ISSN 1976-0485 / eISSN 2234-1315

*Correspondence: ashutofu2020@gmail.com; ashutofu1010@gmail.com

[1] College of Engineering, Wolaita Sodo University (WSU), Wolaita Sodo, Ethiopia

Full list of author information is available at the end of the article

for about 45% of the waste from construction (Gartner & Hirao, 2015; Gaur et al., 2019; Kosmatka et al., 2008; Samad et al., 2016). Among those ingredients, cement (binder) was the most expensive and not eco-friendly. Cements, in a general sense, are adhesive and cohesive materials that are capable of bonding together particles of solid matter into a compact rocklike mass. Above and beyond, cement is a hygroscopic construction material and needs to be stored in a dry, leak-proof, and moisture-proof building. It is advisable to store cement only for 3 months and not beyond that. While, without appropriate storage and beyond the recommended shelf time, this high-energy-consuming resource will turn into an expired and hardened commercial item (Duggal, 2008; Zainudeen & Jeyamathan, 2016). According to several studies on the influence of SCMS on concrete, the significant emissions of greenhouse gases such as CO_2, SOx, and NOx have led to various environmental challenges like global warming, climate change, and desertification. Many components of the cement manufacturing process are potentially harmful to the environment, yet these hazards and opportunities to minimize CO_2 emissions through enhanced energy efficiency are only available for the latter. (Johari et al., 2009; Samad & Shah, 2017; Samad et al., 2016; Yang et al., 2013).

Many types of concrete have been developed for special purposes (Neville & Brooks, 2010). Among them, high-strength concrete (HSC) is substituted for conventional concrete and is utilized in rehabilitating or strengthening concrete structures. HSC, according to ACI 211 4R-08 (ACI 211.4R (ACI Committee) 2008), has a compressive strength of 40N/mm^2 (6000 psi) or greater after 28 days of curing. The use of HSC for applications in structural structures has greatly grown in recent years due to its advantages for the sustainability of our environment by using alternative materials or recycling different industrial and agricultural wastes as supplementary cementitious materials (SCMs) (Alengaram et al., 2010; Samad & Shah, 2017).

Thus, employing SCMs as partial substitutes for clinkers in cement, such as powdered granulated blast furnace slag, fly ash, volcanic ash, metakaolin, and silica fume, can significantly reduce CO_2 emissions and amount of garbage deposited in lake. This makes better use of industrial waste and reduces the amount of clinker in cement, lowering both the use of natural resources and the cost of cement (Awol, 2011; Biswas & Rai, 2020; Deboucha et al., 2017; Prakash et al., 2022; Taffese, 2018; Yang et al., 2013; Yening et al., 2019). Furthermore, SCMs such as ground granulated blast furnace slag, metakaolin, silica fume, and fly ash consumption as a portion of binders for concrete have been increasing all over the world, particularly in the production of high-performance and high-strength concrete. This is because of the potential ability of these materials to improve the performance and properties of concrete through their pozzolanic reaction, along with their filler effect. Additionally, SCMs' inclusion in concrete as mineral admixtures to partially replace cement could serve as an effective means of disposal and somehow preserve the non-renewable resources required to produce cement, because most of them are by-product materials and hence could somehow contribute to sustainable concrete construction. Subsequently, in CI, concrete is mostly used. Moreover, using GGBS at a higher replacement level in cement can significantly reduce concrete costs and pave the path for more cost-effective, environmentally friendly concrete. Therefore, by minimizing the negative impacts of concrete on the environment, CI can achieve sustainability. This can be achieved by replacing partial or all the concrete ingredients such as aggregates and cement with industrial waste (Johari et al., 2009; Majhi & Nayak, 2019; Prakash et al., 2022; Shariq et al., 2013).

In the study conducted by Yening et al., (2019) investigated the recycling of expired cement and aged supplementary cementitious materials based on close packing theory and space filling effect. They concentrated on repurposing old SCMs with expired cement. The tests done to check the suitability of these materials are also limited to microstructure and permeability development, and they blend with other aged SCMs to fill the space between the pastes (Yening et al., 2019). Their study is limited to the finer expired cement, not the hardened expired cement, whereas this study will focus on experimental investigation on bond, microstructure, and durability of those costliest and environmentally unfriendly elements; expired hardened cement blended with ground granulated blast furnace slag as a partial replacement of cement in high-strength concrete; and its compressive, flexural, and split tensile strength; and durability tests. Furthermore, the ultrasonic pulse velocity (UPV) and microstructural characteristics tests are carried out to check concrete quality. Above and beyond, alternatively this research focused, with the intention of reducing both environmental pollution and the total material cost.

2 Experimental Investigation

2.1 Materials

The material properties used for producing concrete mixes are done in the research laboratory as per the related standard code of practice. And in this study, different materials were used, such as cement, fine aggregate, coarse aggregate, water, admixture, expired hardened cement, and GGBS. The *ordinary Portland cement* (Dangote cement) that is produced in Ethiopia (Grade 42.5R), which is available on the market and satisfies the ASTM C150/C150M (2011) standard specification with a specific gravity of 3.14, was used in this research. The *fine*

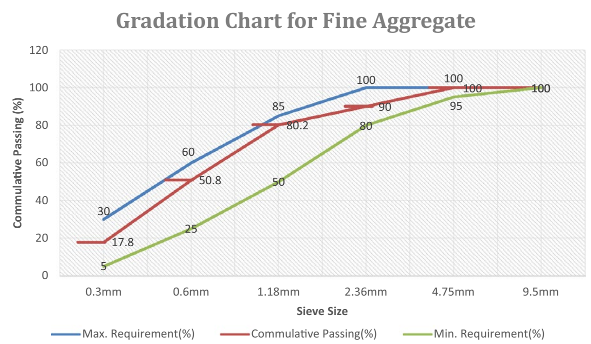

Fig. 1 Gradation chart of fine aggregate

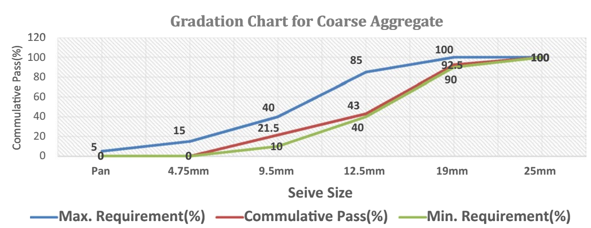

Fig. 2 Gradation chart of course aggregate

aggregate used in this investigation was passed through a 4.75-mm sieve as shown in Fig. 1, and nearby accessible river sand meeting the requirements of the ASTM C33/C33M or ES CD3.201 standard recommendation, and uncontaminated, dried, pure river sand was used. In addition, for more clarification the sieve analysis test result stipulated in Appendix. Thus, the size of the *coarse aggregate* utilized to satisfy the high-strength concrete requirement with a maximum of 19 mm aggregate (size 10–20 mm) as shown in Fig. 2, which was used throughout this experimental investigation. The *water* used in this study for both mixing and curing was supplied by the City of Addis Ababa Water and Sewerage Authority, and was accessible in the laboratory. For this study, *the admixture*, also known as high-range water-reducer admixture, which fits to the ASTM C494/C494M classes of Type F and G water reducers, which are chemically different from the normal water reducers and capable of reducing water content by about 12%.

Materials used as filler that require preparation before use were prepared. *Expired hardened cement* (EHC) was collected from AASTU and *ground granulated blast furnace slag* (GGBS) was obtained from a local Roze Ethiopia PLC, the Ethiopia metals melting factory, which is in Addis Ababa, Kality. Both EHC and GGBS were crushed and ground through marble crushing machines around Kality and sieved through a 75-μm sieve as shown in Figs. 3 and 4, with specific gravity of 2.92 and 2.83, respectively.

2.1.1 Raw Material Characterization

Both the physical and chemical properties of the raw ingredients used in the concrete were studied. The physical properties, including specific gravity, density, particle size distribution, moisture content, and water absorption, were tested for the aggregate.

X-ray fluorescence (XRF) was used to determine the chemical composition of expired hardened cement and GGBS and to realize its compound by Ram J. and Ran B., X-ray diffraction techniques can be used to more accurately determine compound percentages (Singh & Singh, 1995).

Fig. 3 EHC process from source to final preparation to mix

Fig. 4 GGBS process from source to final preparation to mix

Table 1 Chemical composition of EHC and GGBS

S. no.	Chemical composition (%)				
	EHC	GGBS		EHC	GGBS
SiO_2	18.52	54.12	K_2O	< 0.01	0.26
Al_2O_3	4.87	12.65	MnO	0.08	6.40
Fe_2O_3	2.50	4.36	P_2O_5	0.13	0.09
CaO	42.76	5.88	TiO_2	0.14	0.15
MgO	0.76	2.14	H_2O	13.28	0.22
Na_2O	0.14	0.84	LOI	18.00	< 0.01
SiO_2	18.52	54.12	K_2O	< 0.01	0.26

Table 2 Summary of test results for aggregates

Test description	Test results of aggregates	
	Fine	Coarse
Fineness modulus	2.61	2.61
Moisture contents (MC)	2.15%	1.01%
Dry rodded unit weights	1622 kg/m^3	1680 kg/m^3
Specific gravity	2.68	2.84
Water absorption capacity	2%	1.05%

As shown in Table 1, the loss on ignition (LOI) value of EHC is high compared with GGBS. According to Kosmatka and Wilson (2011), the high LOI is due to pre-hydration and carbonation, which may be caused by improper and prolonged storage or alteration during transport or transfer.

2.2 Concrete Mix Proportion

For this experimental investigation, a total of five high-strength concrete mix designs were manufactured. Of those, one mix without SCMs was considered as control. The other four mixes were made by adding 15%, 20%, 25%, and 30% of EHC blended with GGBS by weight as cement replacement. Considering previous literature and their recommended dosage rates of supplementary cementing materials, usually at 5% to 30% or more for cementing material mass (Johari et al., 2009; Kosmatka et al., 2008).

The design mix was done using the ACI mixing procedure "guide for selecting using Portland cement and other cementitious materials" (ACI Committee211, 2008). The concrete was specified to have a slump of 50.8 to 101.6 with a target cubic strength (fcr′) of 48.83 MPa. Several trial mixes were tested prior to the main experimental work in order to achieve the desired mix design. Additionally, the mixed proportion of the control concrete mixes and concrete containing SCMs has specifically expired hardened cement, GGBS, and their quantities used in this study are presented in Tables 2 and 3.

2.3 Concrete Mixing and Fabrication of Specimens

All the *molds* of specified sizes were oiled prior to filling them with concrete, and then specimens were immediately produced. The material was weighed in the required proportions. To keep homogeneity in every concrete mix, cement, EHC, and GGBS were mixed carefully in the initial phase. Then, to form a *dry mix*, sand, and coarse aggregates together with the cementitious materials were mixed for one minute in the concrete mixer. Then they measured the superplasticizer mixed with water. After this, about 80% of the water and superplasticizer mix are added to the mix, and for an additional one minute, mixing continues. Afterward, the remaining water is added and the mix continues mixing for 30 s until the mix becomes uniform in visual inspection. Once the mixing is over, to eliminate segregation, fresh mixed concrete is dropped from less than one meter between mixer and concrete conveyer, then damped concrete were mixed by using a shovel and trowel, until it appears uniform. Subsequently, the slump cone was immediately filled and tamped by using the tamping rod in three layers with 25 strokes for each layer, and the concrete used for slump tests was returned to the mixing pan and, remixed into the

Table 3 Mix proportion and their quantity used in this study

Mix proportion	Mix No	Cement, kg	GGBS, kg	EHC, kg	Fine aggregate, kg	Coarse aggregate, kg	water, kg	Admixture, ml*	W/cm
100% OPC	M Cc	18.7	–	–	19.10	29.83	6.74	51	0.36
85% OPC + 10%GGBS + 5% EHC	M R 1	15.89	1.87	0.935	19.10	29.83	6.74	51	0.36
80% OPC + 10%GGBS + 10% EHC	M R 2	14.96	1.87	1.87	19.10	29.83	6.74	51	0.36
75% OPC + 10%GGBS + 15% EHC	M R 3	14.025	1.87	2.805	19.10	29.83	6.74	51	0.36
70% OPC + 10%GGBS + 20% EHC	M R 4	13.09	1.87	3.74	19.10	29.83	6.74	51	0.36

*Admixture used as ASTM C-494/C 494M recommendation a superplasticizer as 3 ml per one kilogram by weight of cementitious material

Mix_{Cc} = control high-strength concrete mix, M_R 1, 2, 3, and 4 are 15%, 20%, 25%, 30%, respectively, of EHC blended with constant 10% GGBS concrete mix made partial replacement of cement

batch by using a shovel and trowel. Finally, the mixed concrete was poured into the prepared mold with two layers of appropriate compact on a table vibrator for 15 s for each layer.

Later, the specimens were removed from each mold after 24 h and coded for identification, and placed at curing tank until the desired age with a temperature of 20 ± 2 °C and a humidity of 55%. After the desired curing age, the samples are taken out of the curing tank and dried in the air for 18 ± 4 h. at laboratory conditions (at room temperature). As a final point, the specimens of concrete underwent different tests with the intention of evaluating their strength, bond, microstructure, and durability. From the same mix, three samples are taken to calculate the mean value of a particular test sample, which represents the result of that test. In this study, five different mixes were prepared using three different mold sizes, and the specimens used were tested using cube, prism, and cylinder molds. The cube, with a size of 100 × 100 × 100 mm and prism size of 100 × 100 × 500 mm is used for compressive and flexural strength tests, respectively. Additionally, the 100-mm diameter and 200-mm height size of the cylindrical mold are used for split tensile, ultrasonic pulse velocity, and durability (permeability test). Besides, for bond strength tests, cylinders of 100 mm in diameter and 200 mm in height embedded with a 16-mm diameter bar.

2.4 Test Procedures

At the start, the *control mix* is prepared by using basic materials of HSC such as cement, fine and coarse aggregate, water, and HRWRA without SCMs tested for 7-day strength to determine the final proportion of the ingredients. Then, based on the 7-day result, the final mix was designed. Totally, the 90 specimens (30 cubes for compressive, 15 flexural beams, and 45 cylinders for permeability, split tensile, and bond) were cast on five different mixed proportions of C-40 concrete. The test age for the compressive strength of this study was performed at ages 7 and 28 days, whereas all the remaining tests were conducted at the age of 28 only. After all mechanical tests are performed, a sample from the control mix and optimum replacement is taken to conduct microstructure tests on concrete. Above and beyond, the following specific methods are involved as sub-sections.

The *workability* of HSC in this study was assessed through a slump test using ASTM C 143. Additionally, slump tests were conducted for each of the concrete mixes using a standard slump cone with height of 300 mm, a bottom diameter of 200 mm, and a top diameter 100 mm.

Compressive strength was measured as per ASTM C192/192M-07 (2007). According to Newman and Choo (2003), the use of 100-mm cubes is common with high-strength concrete as a means of decreasing the load testing machine's necessary capacity. Hence, in this study test performed, 30 pieces of 100 × 100 × 100 mm cube-sized samples were prepared for both control and mix made with SCMs for C-40 concrete at ages 7 and 28 days. Each concrete's compressive strength was measured by testing the cubes in a 3000-kN capacity standard compression testing machine and by applying a rate of 3.0 $N/mm^2/s$ constant compressive load up to failure.

The *splitting tensile* test is carried out on a standard cylinder with a diameter of 100 mm and a height of 200 mm using a bearing strip of 3 mm plywood that is free of imperfections and is about 30 mm wide. The split tensile strength of each concrete was determined by the cylindrical specimens in a 3000-kN capacity standard compression testing machine, applying load after the specimen is aligned on the machine, and by the 5.0$N/mm^2/s$ rate till failure according to the ASTM C 496 standard test method for splitting tensile strength.

Flexural strength was measured as per the ASTM C 78 concrete flexural strength test method. Hereafter, 15 pieces of 100 × 100 × 500-mm prism specimens were prepared for both control and mix made with SCMs for C-40 concrete for flexural strength testing after 28 days curing. Each concrete flexural strength was determined by testing the prism specimens in a 100-kN capacity standard machine for flexural testing and by a 20.0N/mm^2/s rate till failure.

By the side of *Bond strength*, three-cylinder mold sizes of 100*200 mm for each mix were prepared by inserting normal strength deformed reinforcement bars available in the local market of 16 mm in diameter and 900-mm-long vertically along each cylinder at the central alignment. To control the embedment length and cut the bond near the loaded area of the specimen, plastic conduits were introduced. Thereafter, the 28-day bond strength was evaluated by performing a direct pull-out test in a center-hole jack to measure the applied load. Meanwhile, the load was applied manually, and the loading rate was not entirely kept constant. But the loading rate was kept below 2.75kN/s for all experiments. The average bond stress was calculated from the maximum applied axial load using Eq. (1):

$$\tau = \frac{P}{\pi \mathrm{LeDb}}, \quad (1)$$

where τ = average bond stress (MPa), P = maximum applied axial tension force (N), Le = embedment length (mm), and Db = diameter of bar (mm).

A durability or permeability test of HSC was carried out at 28 days on 100-mm diameter and 200-mm height cylinders by applying non-steady water penetration. The steps followed for conducting water penetration tests are: primarily, the test samples were assembled in the permeability apparatus and 3 bar (0.3 MPa) pressure was applied for the first 24 h. Then 5 bar (0.5 MPa) of water pressure was applied for the next 24 h. Thirdly, the water pressure was increased to 7 bar (0.7 MPa) for the third 24 h, for a total of 72 h under pressure. Finally, toward the end of 72 h, the concrete cubes were removed from the permeability rig and split in two using a tensile splitting machine. Upon visual examination, the portion of specimens into which water penetrates appears darker than the rest. Then the darker zone was marked and water penetration depth measurements were taken.

Scanning electron microscopy (SEM) analysis was done at Adama Science and Technology University (ASTU), Adama, Ethiopia. The SEM analysis was done after the 28-day water-cured concrete samples were tested for compressive strength. Sample fragments were gathered and crushed as powder and sieved through 75 µm and images were obtained using the secondary electron image mode. Furthermore, the machine used was the JCM-6000 plus Bench Top SEM JEOL machine.

The *ultrasonic pulse velocity test* (UPV) is one of the non-distractive test methods that is conducted by the emission of waves through the test specimens (Kosmatka et al., 2008; Shariq et al., 2013). The ultrasonic tester consists of two transducers (one transmitter and one receiver head, 54 kHz type), two connecting cables, one calibration rod, one bottle of coupling agent for optimal surface contact, and two 1.5 V alkaline D-type batteries that make up the UPV tester. Furthermore, in UPV, transducers are often arranged in three ways: direct (opposite faces), semi-direct (adjacent faces), and indirect (the same face). Because the longitudinal pulses leaving the transmitter are propagated in the direction normal to the transducer face, the direct transmission method was used to determine the pulse velocity V in this study. The UPV tests were carried on a diameter of 100 mm and a height of 200 mm cylinders as per the guidelines of ASTM C 579–02. Afterward, the pulse velocity is calculated by using Eq. (2):

$$V = \frac{L}{T}, \quad (2)$$

Table 4 Summary of laboratory tests conducted in this study

Laboratory tests	Standards	Reference no.	Laboratory tests	Standards	Reference no.
Sieve analysis	ASTM C33	ASTM C33/C33-M-08, 2008a)	Workability	ASTM C143	ASTM C143/C143M-08, 2008c)
Aggregate specific gravity and absorption of	ASTM C127 and C128	ASTM C127-07, 2007a; ASTM C128–07a, 2007b)	Compressive strength	ASTM C192	ASTM C192/C192M-07, 2007)
			Flexural strength	ASTM C78	ASTM C78-08, 2008d)
Moisture content	AASHTO T255	AASHTO T255, 2000)	Spilt Tensile	ASTM C496	ASTM C496/C496M-04, 2004b)
Normal consistency	ASTM C187	ASTM C187-04, 2004a)	Bond (pullout)	ASTM C900	ASTM C900-06, 2006)
Setting time	ASTM C191	ASTM C191-08, 2008b)	Ultrasonic pulse velocity	ASTM C579 and IS:13311–1	ASTM C597-16, 2016; IS:, 133112002, 1992)

Table 5 Average slump test result of concrete with control mix and EHC blended with GGBS

S. no.	Mix proportion of paste	Slump value*(mm)
1	100% OPC	90
2	85% OPC + 10%GGBS + 5% EHC	91.5
3	80% OPC + 10%GGBS + 10% EHC	94
4	75% OPC + 10%GGBS + 15% EHC	97.5
5	70% OPC + 10%GGBS + 20% EHC	100.5

* Slump value (mm) with water/cement ratio of 0.36 including 3 ml/kg of HRWRA

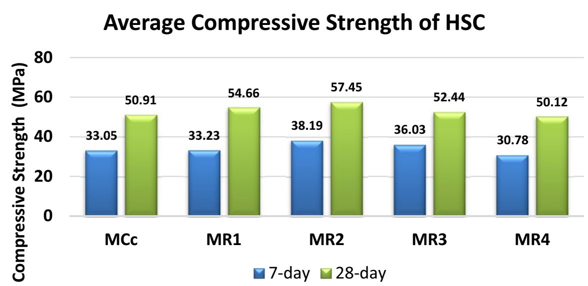

Fig. 5 Compressive strength test result

where V = pulse velocity, m/s; L = distance between centers of transducer faces, m; and T = transit time, s.

All the tests were carried out according to the standards and with their references given in Table 4.

3 Results and Discussion

3.1 Influence of EHC Blended with GGBS on Workability of HSC

According to ACI 211.4R-93 (ACI Committee211, 2008) and ACI Committee 116, in general, it is possible for HSC at slumps of an extra 177.8 mm with superplasticizer without segregation to be properly handled, consolidated, and commonly placed at the lowest slump. Moreover, the workability and strength of concrete are influenced by the quality of concrete-making constituents.

Table 5 shows that the slump value increases with increasing the EHC blended with GGBS content. Moreover, it shows that the fresh concrete slump value of all the blends is in the range of specification of 90–103 mm, which is characterized by high workability. This workability value is attained at a 0.36 water cement ratio, including 3 ml/kg of HRWRA, together with those blends. Its additional distinguishing feature is that the control mix workability is low as equated to the other mix. This, increase in workability, is probably due to high content of the water (H_20) in EHC as shown in Table 1. Moreover, high-range admixtures used are to give increased workability and a higher rate of slump loss.

3.2 Influence of EHC Blended with GGBS on Compressive Strength of HSC

The influence of 15%–30% partial replacement of cement by EHC blended with GGBS on the compressive strength at 7 and 28 days is presented in Fig. 5. According to ACI 318M-02, the 7-day concrete compressive strength is 2/3 or 67% of the cubes' target mean strength after 28 days. Consequently, cubes' compressive strength at 7 days should be greater than 32.55 MPa (0.67*48.83 = 32.55 MPa). Hence, for this study, the targeted 7-day control mix compressive strength used for comparison was 32.55 MPa.

The result from Fig. 5 reveals that, from the 7th day of compressive strength, there are positive and negative raises of the target mean strength. Primarily, a positive increment was achieved with up to 25% (to be exact, 0.55%, 9.02%, and 15.55% with 15%, 20%, and 25% of EHC blended with GGBS, respectively) cement partial replacement compared to the control mix. Inversely, the reduction in compressive strength attained at MR4 (30% replacement of OPC by EHC blended with GGBS) is inverse. Furthermore, from Fig. 5, we easily realize that the fall of the 7th day compressive strength starts from MR3, but it results in a higher than the target strength up to MR4.

Whereas the 28th day compressive strength result shown in Fig. 5 is like the 7th day result both positive and negative increment. The first three mixes, such as MCc, MR1, MR2 and MR3, show a positive increment from the standard or target mean strength (48.83 MPa), but MR4 shows a reduction from the control mix. Moreover, the whole mixes satisfy the recommended target mean strength or are all greater than 48.83 MPa. Predominantly positive increments were achieved, up to 25% replacement, specifically 7.37%, 12.85%, and 2.97% with 15%, 20%, and 25% of EHC blended with GGBS, respectively, compared to control mix. On the other hand, the reduction in compressive strength attained at MR4 with 30% replacement of OPC by EHC blended with GGBS and a loss of 1.55% from the control mix. Furthermore, from Fig. 5 we easily realize that the fall of the 28th day compressive strength starts at MR3, but it results is higher than the target strength up to MR4. This, the fall of the 28th day compressive strength, implies that the compressive strength of concrete in which partial replacement of OPC by EHC blended with GGBS decreases the mixture of cement content, which leads to a fall in the hydration reaction necessary for concrete strength development. In the study conducted by (Johari et al., 2009), their results reveal that the different SCMs' addition influences the HSC compressive strength of mixes and their development of strength would need the OPC hydration rate plus the reaction between calcium hydroxide, Ca (OH)2 and SCMs (Johari et al., 2009). According to Dave et al. (2017) (Singh & Singh, 1995) when a less reactive pozzolan is employed in OPC, composed of one more reactive, the result is greater than those tested in the binary mixtures. There is a combined effect between these pozzolans; this outcome is called a synergic effect. Moreover, in the study conducted by Yening et al. (2019) (Yening et al., 2019), another significant reason for the lower strength of the hardened mortar prepared from aged raw materials is inhomogeneity; whereas, in this study, the reason for the lower MR4 is probably as a result of the inclusion of a high amount of expired harden cement.

The higher compressive strength value among the entire mix of EHC blended with GGBS was MR2 with 20% replacement of OPC by EHC by GGBS, which shows higher compressive strength improvement than the control mix with 15.55% and 12.85% for the 7th day and 28th day cured HSC, respectively. GGBS are referred to as "active pozzolans" (Prakash et al., 2022). It was observed that supplementary cementitious materials appeared to have an articulated impact on compressive strength. And this excellent performance of GGBS absolutely proved its pozzolanic reaction (i.e., compressive strength) was still effective especially on the microstructure filled by pozzolanic hydration products. Observations show that there is a consistent increase in compressive strength with an increment in the level of supplementary cementitious materials in the blend. These GGBS (cementitious powders) can be well blended to form an optimal arrangement and offset disadvantages from relatively lower hydraulic property of expired harden cement. This improved CSH and decreased the amount of water that remained after hydration with the addition of certain substances as well. In essence, it decreased the bigger water-filled holes and improved the material's strength.

3.3 Influence of EHC Blended with GGBS on Split Tensile Strength of HSC

Fig. 6 shows, at the age of 28 days, the rate of splitting tensile strength development of 0%, 15%, 20%, 25%, and 30% of EHC blended with GGBS. And the rate of splitting tensile strength development was 4.13 MPa, 4.54 MPa, 4.89 MPa, 4.38 MPa, and 4.07 MPa of 0%, 15%, 20%, 25%, and 30% of EHC blended with GGBS, respectively. Moreover, like compressive strength, both positive and negative influences are observed from the control mix. Increments were achieved on a mix of MR1, MR2 and MR3 with increments of 9.93%, 18.4% and 6.05%, respectively, whereas the reduction in strength achieved in MR4 mixes was a 1.45% reduction from the control mix.

According to some scholars, different pozzolanic materials have different effects on strength. But most of them, including GGBS, have been found to improve the strength of concrete, especially in the latter days (after 28 days) (Abebe, 2002; Neville & Brooks, 2003). The results from this study also show that the split tensile strength of high-strength concrete is improved by up to 25% by the replacement of cement by EHC blended with GGBS from the reference concrete mix, but reduced when the replacement percent is increased to 30%. The results show, the addition of GGBS 10% seems a favorable way to improve the expired cement hydration, which even possibly increases the split tensile strength.

3.4 Influence of EHC Blended with GGBS on Flexural Strength of HSC

In this study, the test was performed for 28 days with 0%, 15%, 20%, 25%, and 30% of EHC blended with GGBS added to the high-strength concrete as cement partial replacement. As shown in Fig. 7, the flexural strength development of 0%, 15%, 20%, 25% and 30% of EHC blended with GGBS added to the high-strength concrete as partial replacement of cement was 5.62 MPa, 5.95 MPa, 6.29 MPa, 5.76 MPa, and 5.35 MPa, respectively. The normal-weight concrete flexural strength is

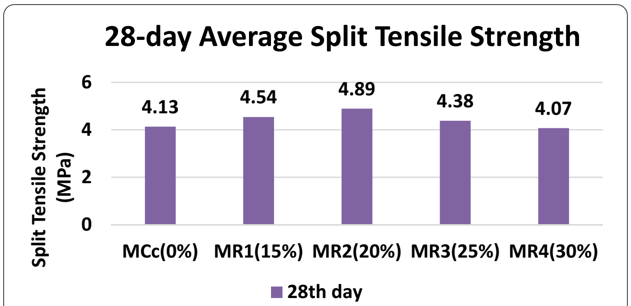

Fig. 6 Split tensile strength test result

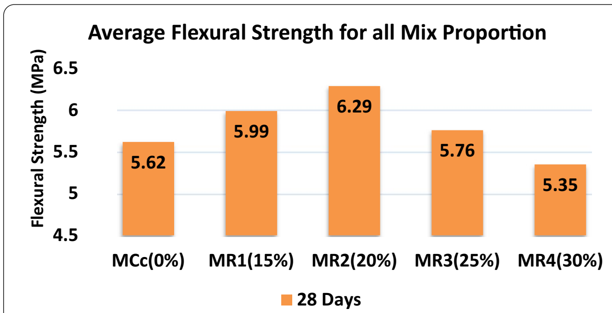

Fig. 7 Flexural strength test result

frequently estimated as 0.7 up to 0.8 times the square root of the compressive strength in megaPascal (MPa) (Kosmatka et al., 2008). Henceforth, all the above flexural strength test results fulfill the requirements of the C-40 grade concrete requirement (that is equal or higher than 5.59 MPa), except the one with 30% EHC blended with GGBS replacement.

In the study conducted by (Dave et al., 2017), they observed that SCMs appeared to have a noticeable influence (namely positively and negatively) on flexural strength. Therefore, the result of this study also reveals that the rate of flexural strength development is positively and negatively influenced with and without SCMs (namely EHC blended with GGBS). The positive influence results are that 15% EHC blended with GGBS concrete improved by 0.37 MPa or 6.58% from 0% (control mix concrete), 20% EHC blended with GGBS improved by 0.67 MPa or 11.92% from control, and 25% EHC blended with GGBS improved by 0.14 MPa or 2.50% from control; whereas, negative influence result was achieved in the mix with 30% EHC blended with GGBS replacement and the reduction with 0.27 MPa or 4.80% from 0% or control mix. Like compressive strength, MR2 (20% replacement of EHC with GGBS) shows higher flexural strength with a 11.92% improvement than the control mix.

3.5 Influence of EHC Blended with GGBS on Bond of HSC

Table 6 clearly shows the inclusion of EHC blend with GGBS in concrete improves the bond strength by up to 20%, besides lower the bond strength when blend content is increased to 25% and 30%. To be precise, at the age of 28 days, the rate of bond strength improvement of 0.70 MPa and 1.17 MPa is 15% and 20%, respectively. Contrarily, the reduction in bond strength achieved at 25% and 30% of EHC blended with GGBS with a negative 0.06 MPa and 0.22 MPa, respectively. As specified and defined by different scholars, splitting failure is characterized by the splitting of the concrete specimen in a brittle mode of failure, especially when both transverse and longitudinal cracks are observed at failure (Ngugi et al., 2014; Qasim & Ahmed, 2018). Also, as shown in Fig. 8A and observed after testing, the all-pull-out specimens have failed by splitting after maximum load.

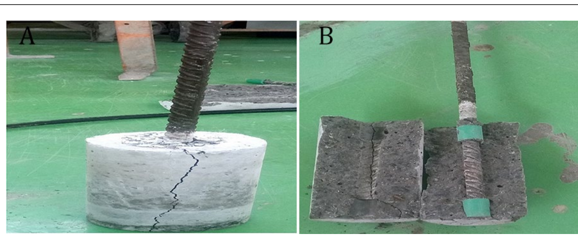

Fig. 8 Pullout test result: **a** crack pattern of specimen, and **b** specimens after splitting

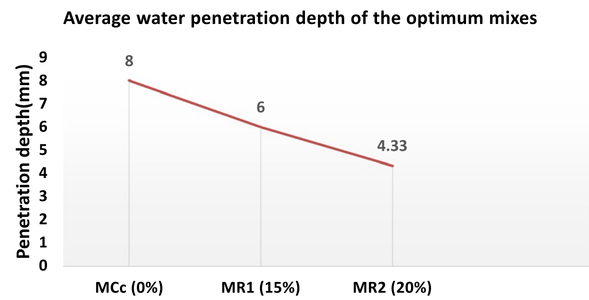

Fig. 9 Average water penetration depth of HSC

3.6 Influence of EHC Blended with GGBS on Water Permeability of HSC

The reading from the 28-day water cured, 3-day water pressure applied and split cylindrical specimen, the maximum and average water permeability, and the variation in permeability through percentage replacement are stipulated. Concrete permeability refers to the number of transmittable fluids or water migration through concrete when the water is under pressure or to the ability of concrete to resist penetration by water or other substances (liquid, gas, or ions) (Birhanu, 2007; Kosmatka et al., 2008). Henceforward, for assessing the influence related to durability due to the replacement of cement by EHC blended with GGBS in HSC with different mix proportions, a non-steady state water permeability test was conducted. As presented in Fig. 9, the replacement of cement by EHC blended with GGBS has a significant influence on the water permeability of HSC. Subsequently, the permeability depth of MR1 and MR2 was reduced compared with control mix (MCc). This is due to the addition of SCMs in concrete. Henceforward, the permeability of concrete decreased with increasing the percent replacement of cement by EHC blended with GGBS. In the previous study, the same effect of SCMs' inclusion in concrete is presented by (Majhi & Nayak, 2019) When GGBS is used, the depth of permeability of concrete gradually decreases.

Neville and Brooks (2010) specify depth of penetration and its relation with permeability. If water penetration depth in the concrete is less than 50 mm, the concrete is generally classified as impermeable; and if the penetration depth is less than 30 mm, it is classified as impermeable under aggressive conditions. Based on this, the concrete produced using EHC blended with GGBS with replacement up to 20% of OPC was that the maximum

Table 6 Average bond stress of HSC

S. no.	Specimen mix code	Nominal bar diameter (mm)	Embedment length (mm)	Maximum axial load, P_{max} (kN)	Average bond stress, τ(MPa)
1	MCc	16	200	73.77	7.34
2	MR1	16	200	80.86	8.04
3	MR2	16	200	85.52	8.51
4	MR3	16	200	73.16	7.28
5	MR4	16	200	71.55	7.12

Table 7 The average and maximum water penetration depth of the optimum mixes

S. no.	Mix code and percentage replacement	Penetration depth(mm)	
		Maximum	Average
1	MCc (0%)	10	8
2	MR1 (15%)	9	6
3	MR2 (20%)	7	4.33

water penetration depth of concrete up to 20% replacement is less than 30 mm, which is 10 mm as shown in Tables 6 and 7, since the high-strength concrete produced by using EHC blended with GGBS was impermeable under aggressive conditions.

Moreover, the other researchers stated the durability of concrete as a function of permeability, and high strength and low permeability are linked to one another because high strength requires a low volume of pores (Awol, 2011). As water represents the most important liquid among those penetrating through concrete, improvement in the impermeability of concrete to water implies improvement in the durability of concrete. Henceforth, the durability of concrete up to 20% replacement of EHC blended with GGBS improves water penetration (durability) of HSC. This reduction in water depth indicates the formation of fewer pores in concrete and may be attributed to the filling of concrete void spaces by the fines of GGBS. Once voids are occupied, concrete becomes compact, leaving no space for water to penetrate.

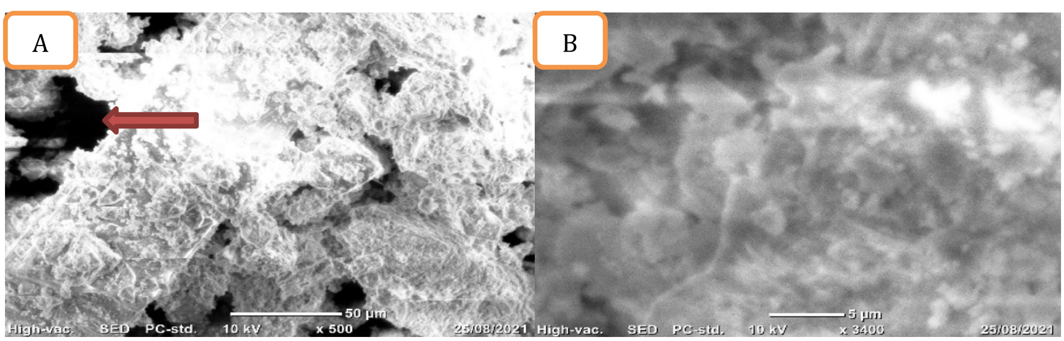

Fig. 10 SEM image of row control mix (100% OPC) at different magnification rate **a** at magnification rate 50µm, and **b** at magnification rate 5 µm

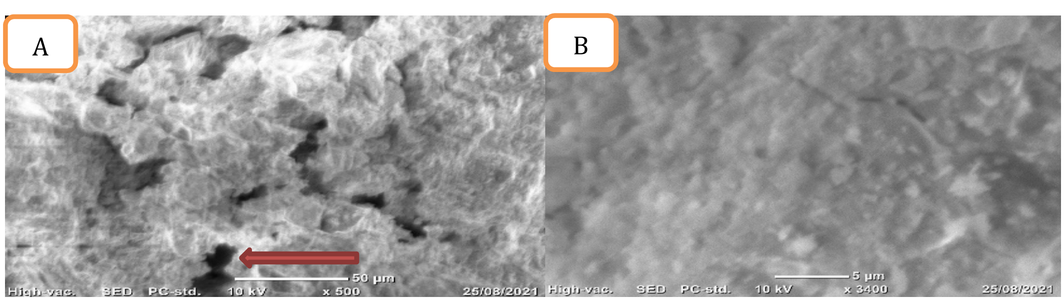

Fig. 11 SEM image of row MR2 mix (80% OPC and 20% EHC blended with GGBS) at different magnification rate **a** at magnification rate 50µm, and **b** at magnification rate 5 µm

3.7 Influence of EHC Blended with GGBS on Microstructure of HSC

3.7.1 Scanning Electron Microscopy (SEM)

Concrete paste samples SEM micrographs are taken in order to study the different hydration products arrangements such as calcium hydroxide, CSH gel, and un-hydrated cement or expired hardened cement or GGBS particles inside the concrete paste sample. A sample for SEM was taken from compressive strength tests performed, and a sample from control mix and optimum replacement was taken to conduct microstructure tests on concrete.

Figs. 10A and 11A clearly show the void space of the hydrated particles, but their extent is different at the same magnification rate. When we realize from control mix Fig. 10A, the large void space of hydrated particles is observed, whereas in Fig. 11A mix with 20% SCMs, the extent of void is lower than that of control. This shows the inclusion of EHC blended with GGBS in concrete fills the void between hydrated particles and proves densification of the microstructure. Other scholars have noted the same findings. Previous studies on the filling effect of SCMs showed that the filler action involves incorporating supplementary materials that are finer than the OPC, so that these occupy small pores previously left vacant. Moreover, they also lead to the densification of the microstructure and increase compressive strength (Dave et al., 2017).

Then again, in Figs. 10B and 11B, we clearly realize the bond between hydrated particles. The control concrete mix shown in Fig. 10B is less bonded or little pores are recognized, while in Fig. 11B the concrete containing those blends is closely packed and improves the bond between the hydrated particles. Moreover, Fig. 11B shows the compact microstructure of the concrete sample as compared to that of the Fig. 10B sample, mostly due to the filling effect of the fine un-hydrated particles of GGBS. The results from Yening et al. (2019) deeply certified that the hydrating activities of expired cement and filling effects of aged SCMs, and the blending of aged SF and SG successfully replaced an equivalent amount of expired cement without impacting the microstructure, which might reveal the potential of expired cement as a kind of supplementary material. (Yening et al., 2019).

Once hydration process is formed the C-S-H gel fill the pores and prevents permeability which makes the concrete durable. Besides, the overall microstructure is very compact, i.e., the hydrated particles are all connected and the overall pore size in the microstructure is exceptionally reduced. Above and beyond, in the existence of EHC blended with GGBS, a very dense matrix is seen, which shows its effectiveness over OPC. The presence of finely grounded pozzolanic materials leads to the densification of the microstructure and, as a result, the concrete strength, bond, and durability are improved.

3.8 Influence of EHC Blended with GGBS on the Ultrasonic Pulse Velocity of HSC

An ultrasonic pulse velocity (UPV) for concrete is generally prepared to check the concrete quality by determining an ultrasonic pulse velocity passing through the structure of concrete. And, the UPV value is used as an indicator of the microstructure development of concrete (Biswas et al., 2021). Moreover, UPV determines the homogeneity, strength, internal flows, trapped air, cracks, segregation, honeycombing, workmanship, compaction, and durability of concrete. In this test method, high velocity results notice the concrete is good, whereas lower velocity notices the cracks and voids.

Use of SCMs, such as GGBS, SF, MK, and FA, is helpful in increasing its resistance against penetration of moisture content and making denser concrete structures (Dave et al., 2017). Hence, from Table 8, and based on IS: 13311-part 1 (IS:, 13311-2002, 1992), UPV test results of entirely the blends of EHC and GGBS have revealed good to excellent velocity, which indicates that the microstructure of concrete is denser and increases moisture penetration resistance.

A study on the assessment of NDT in high-strength concrete incorporating SCMs composites showed that including SCMs in concrete has an influence on compressive strength that is fairly correlated irrespective of the ultrasonic pulse velocity (Khan, 2012). The results of this study also reveal that the pulse velocity result is correlated to compressive strength too. Therefore, the

Table 8 Average UPV test result for cylinder sample

Mix code	Average pulse time (μsec), *T*	Length of cube (mm), *L*	UPV (mm/μsec) $V = L/T$	Concrete quality based on IS: 13311-part 1
MCc	46.7	200	4.28	Good
MR1	44.5	200	4.50	Excellent
MR2	44.2	200	4.52	Excellent
MR3	46.1	200	4.33	Good
MR4	46.8	200	4.27	Good

introduction of EHC blended with GGBS into concrete influences both the ultrasonic pulse velocity and compressive strength in a similar way.

As described by Steven et al. (Kosmatka et al., 2008), a non-distractive test program is probably carried out for a range of purposes with regard to the hardened concrete strength, including: in-place concrete strength determination, monitoring concrete strength gain rate, no homogeneity location, such as voids or honeycombing in concrete, relative strength determination of comparable members, concrete cracking evaluation and delamination, damage from mechanical or chemical forces evaluation, location of steel reinforcement, size, and corrosion activity and dimensions of member (Kosmatka et al., 2008). Hence, all the factors listed are directly or indirectly related to the strength, microstructure, bond, and durability of concrete. Likewise, the result of UPV shows good and excellent, so the concrete containing EHC and GGBS, strength, microstructure, bond, and durability are also good and excellent.

4 Conclusion

The current study was conducted to investigate the influence of EHC blended with GGBS as a partial replacement of cement on the bond, microstructure, and durability of high-strength concrete. It was found that the blending of EHC and GGBS successfully replaced an equivalent amount of cement up to a 25% replacement without impacting the microstructure, which might reveal the potential of the EHC blend with GGBS as a kind of SCM. Therefore, it is possible to conclude that:

1. The *compressive strength* of OPC by EHC blended with GGBS concrete increases with the addition of those bled up to 25%, and the improvement in strength indicates that the pozzolans are more effective. Moreover, the result from both the 7th day and 28th day compressive strength tells us that there are positive and negative increments of the target mean strength. The optimum mix, MR2, with 20% replacement of OPC by EHC blended with GGBS, has shown 15.55% and 12.85% higher compressive strength than the control mixes on the 7th day and 28th day of cured HSC, respectively.
2. The results from *flexural and split tensile strength* of HSC also show that the sound improved up to 25% by replacement of cement by EHC blended with GGBS from the reference concrete mix, whereas a reduction in strength was achieved in MR4 mixes from the control mix. Henceforth, all flexural and splitting tensile strength test results fulfill the requirements of the C-40 grade concrete requirement, except the one with 30% EHC blended with GGBS replacement.
3. The inclusion of the EHC blend with GGBS in concrete failed by splitting, and improvement and reduction of the bond strength were achieved; improvement of up to 20% was achieved, besides lowering the bond strength when the blend content was increased to 25% and 30% at the age of 28 days. Moreover, with a percent of bond strength improvement of 9.54% and 15.94%, respectively, Contrarily, the reduction in bond strength achieved at 25% and 30% of EHC blended with GGBS with a negative percent reduction was 0.82% and 2.99%, respectively.
4. In all cases, the *water permeability* of EHC blended with GGBS concrete has shown acceptable results. With an increase in the percentage of SCMs on the 28th day, water permeability in concrete decreases due to the higher surface area of the cementitious material used in the binder. This points out that the inclusion of EHC blended with GGBS in HSC makes it more durable as compared to plain concrete.
5. The overall microstructure of the control specimen is densely precipitated, but a couple of pores are noticeable; whereas, in a mix with 20% SCMs, the extent of void is lower than that of control. This shows the inclusion of EHC blended with GGBS in concrete fills the void between hydrated particles and proves densification of the microstructure. This leads to a higher density of the concrete in the microstructure, and thus the strength, bond, and durability improve.
6. The ultrasonic pulse velocity results show that on all mixtures of SCMs, such as EHC and GGBS, the concrete microstructure is denser and helpful in increasing its resistance against moisture content penetration. Henceforth, all the combinations have shown good to excellent velocity, which indicates that the utilization of EHC blended with GGBS makes the concrete structure denser and increases its resistance against moisture penetration. The result of introducing EHC blended with GGBS reveals that the pulse velocity result is correlated to strength bond and durability too.
7. Based on the test results, the optimum mixes in all strength and durability aspects of concrete were mix MR2 with a mix proportion of 20% as partial replacement to cement by EHC blended with GGBS. Hence, employment of EHC blended with GGBS in HSC could be the best replacement for cement, and would help in decreasing the load on natural resources and supporting the utilization of waste materials in construction.

Appendix

See Tables 9 and 10

Sieve Analysis and Fineness Modules of Aggregate

Table 9 Sieve analysis of coarse aggregate

Sieve size	Weight of sieve (gm)	Weight of sieve and retained (gm)	Weight of retained (gm)	Percentage retained (%)	Cumulative retained (%)	Cumulative passing (%)	Specification limit ASTM C 33
25 mm	1090	1090	0	–	–	100	100
19 mm	1230	1380	150	7.5	7.5	92.5	90–100
12.5 mm	1210	2200	990	49.5	57	43	40–85
9.5 mm	1140	1570	430	21.5	78.5	21.5	10–40
4.75 mm	1240	1670	430	21.5	100	0	0–15
Pan	990	990	0	–	–	–	0–5
Total			2000		243		

Table 10 Sieve and fineness modulus of fine aggregate

Sieve size	Weight of sieve (gm)	Weight of sieve and retained (gm)	Weight of retained (gm)	Percentage retained (%)	Cumulative retained (%)	Cumulative passing (%)	Specification limit ASTM C 33
9.5 mm	1140	1140	0	–	–	100	100
4.75 mm	1240	1240	0	–	–	100	95–100
2.36 mm	1160	1210	50	10	10	90	80–100
1.18 mm	1050	1099	49	9.8	19.8	80.2	50–85
600 µm	1020	1167	147	29.4	49.2	50.8	25–60
300 µm	900	1065	165	33	82.2	17.8	5–30
Pan	990	1078	88	17.6	99.8	0.2	0–10
9.5 mm	1140	1140	0	–	–	100	100
Total			499		261		

$$\textbf{Fineness modulus(FM)} = \frac{\sum \text{Cumulative retained}}{100},$$
$$\text{FM} = \frac{243}{100} = 2.43.$$
$$\textbf{Fineness modulus} = \frac{\sum \text{Cumulative retained}}{100},$$
$$= \frac{261}{100} = 2.61.$$

Acknowledgements
The authors would like to thank China State Construction Engineering Corporation (CSCEC), Addis Ababa Institute of Technology (AAIT), Adama Science and Technology University (ASTU) and Addis Ababa Science and Technology University (AASTU) for their provision of laboratory facilities, and all laboratory technicians, individually Mr. Yemanebrehan Emiru, during this work. The authors would also like to take this chance to appreciate and acknowledge all the organizations and people who played a role, professionally and personally, in the completion of this thesis. Mr. Mehari W/Gebriel for his committed permission to the preparation of materials by their marble grinding machine, and YENCOMAD CON. PVT. LTD. CO., Bole Kotebe, Addis Ababa, for their coarse aggregate provision.

Author contributions
All the listed three authors have their own contribution for this research regarding to their arrangement. All authors read and approved the final manuscript.

Authors' information
Ashenafi Tofu Chofore is Lecturer, at College of Engineering, Wolaita Sodo University (WSU), Wolaita Sodo, Ethiopia.
Dr. Bahiru Bewket Mitike is Assistant professor at Adama Science & Technology University, Department of civil Engineering, Adama, 1888, Ethiopia.
Abenezer Tariku Haile is Lecturer, at College of Architecture and Civil Engineering, Addis Ababa Science and Technology University (AASTU), Addis Ababa, Ethiopia.

Funding
Not applicable.

Availability of data and materials
All materials and data are available on the hands of the authors.

Declarations

Ethics approval and consent to participate
Not applicable.

Consent for publication
Not applicable.

Competing interests
The authors declare that there are no conflict of interest concerning the publication.

Author details
[1] College of Engineering, Wolaita Sodo University (WSU), Wolaita Sodo, Ethiopia. [2] Department of Civil Engineering, Adama Science & Technology

University, 1888 Adama, Ethiopia. [3]College of Architecture and Civil Engineering, Addis Ababa Science and Technology University (AASTU), Addis Ababa, Ethiopia.

Received: 20 March 2022 Accepted: 11 September 2022
Published online: 17 November 2022

References

AASHTO T 255. (2000). Standard method of test for total evaporable moisture content of aggregate by drying, 2000.

Abebe, D. (2002). *Construction materials laboratory manual*. Addis Ababa University Printing Press.

ACI Committee 211. (2008a). *Guide for selecting proportions for high-strength concrete using Portland cement and other cementitious materials*. American Concrete Institute.

ACI 211.4R (ACI Committee). (2008b). *Guide for selecting proportions for high-strength concrete using portland cement and other cementitious materials*. American Concrete Institute.

Alengaram, U. J., Mahmud, H., & Jumaat, M. Z. (2010). Comparison of mechanical and bond properties of oil palm kernel shell concrete with normal weight concrete. *International Journal of the Physical Sciences., 5*(8), 1231–1239.

Andal, J., Shehata, M., & Zacarias, P. (2016). Properties of concrete containing recycled concrete aggregate of preserved quality. *Construction and Building Materials., 30*(125), 842–855.

ASTM C187-04. (2004a). *Standard test method for normal consistency of hydraulic cement*. ASTM International.

ASTM C496/C496M-04. (2004b). *Standard test method for splitting tensile strength of cylindrical concrete specimens*. ASTM International.

ASTM C900-06. (2006). *Standard test method for pullout strength of hardened concrete*. ASTM International.

ASTM C192/C192M-07. (2007). *Standard practice for making and curing concrete test specimens in the laboratory*. ASTM International.

ASTM C127-07. (2007a). *Standard test method for density, relative density (specific gravity), and absorption of coarse aggregate*. ASTM International.

ASTM C128-07a. (2007b). *Standard test method for density, relative density (specific gravity), and absorption of fine aggregate*. ASTM International.

ASTM C33/C33M-08. (2008a). *Standard specification for concrete aggregates*. ASTM International.

ASTM C191-08. (2008b). *Standard test methods for time of setting of hydraulic cement by vicat needle*. ASTM International.

ASTM C143/C143M-08. (2008c). *Standard test method for slump of hydraulic-cement concrete*. ASTM International.

ASTM C78-08. (2008d). *Standard test method for flexural strength of concrete (using simple beam with third-point loading)*. ASTM International.

ASTM C150-11. (2011). *Standard Specification for Concrete Aggregates*. West Conshohocken, PA: ASTM International

ASTM C597-16. (2016). *Standard Test Method for Pulse Velocity Through Concrete*. ASTM International.

Awol, A. (2011). *Using marble waste powder in cement and concrete production*. Addis Ababa University School of Graduate Studies.

Bao, L., Shi, C., Zhang, J., & Wang, J. (2018). Effects of carbonated hardened cement paste powder on hydration and microstructure of Portland cement. *Construction and Building Materials, 186*, 699–708.

Birhanu B. (2007). Comparison of Concrete Durability as Produced by Various Cements Manufactured in Ethiopia, *M.Sc. Thesis,* Addis Ababa University School of Graduate Studies.

Biswas, R., & Rai, B. (2020). Effect of cementing efficiency factor on the mechanical properties of concrete incorporating silica fume. *Journal of Structural Integrity and Maintenance, 5*(3), 190–203.

Biswas, R., Rai, B., & Samui, P. (2021). Compressive strength prediction model of high-strength concrete with silica fume by destructive and non-destructive technique. *Innovative Infrastructure Solutions, 6*(65), 1–14.

Dave, N., Misra, A. K., Srivastava, A., Sharma, A. K., & Kaushik, S. K. (2017). Study on quaternary concrete micro-structure, strength, durability considering the influence of multi-factors. *Construction and Building Materials., 139*, 447–457.

Deboucha, W., Leklou, N., Khelidj, A., & Oudjit, M. N. (2017). Hydration development of mineral additives blended cement using thermogravimetric analysis (TGA): Methodology of calculating the degree of hydration. *Construction and Building Materials., 15*(146), 687–701.

Duggal, S. K. (2008). *Building materials (Third Revised Edition)*. New Age International (P) Limited, Publishers.

Gartner, E., & Hirao, H. (2015). A review of alternative approaches to the reduction of CO2 emissions associated with the manufacture of the binder phase in concrete. *Cement and Concrete Research., 1*(78), 126–142.

Gashahun, A. D. (2020). Assessment on cement production practice and potential cement replacing materials in Ethiopia. *Civil and Environmental Research, 12*(1), 22. ISSN 2224-5790 (Paper) ISSN 2225-0514 (Online).

Gaur, A., Sharma, R., Srivasatava, S., Singh, G., & Kumar, V. (2019). An experimental study of comparison of strength of glass fibre reinforced and conventional concrete of M-30 grade. *International Journal of Scientific Research and Review, 07*(03), 1239.

IS: 13311-2002. (1992). *Method of non-destructive testing of concrete-methods of test, Part 1*. CED 2: Cement and Concrete.

Johari, M. M., Brooks, J. J., Kabir, S., & Rivard, P. (2011). Influence of supplementary cementitious materials on engineering properties of high strength concrete. *Construction and Building Materials., 25*(5), 2639–2648.

Khan, M. I. (2012). Evaluation of non-destructive testing of high strength concrete incorporating supplementary cementitious composites. *Resources, Conservation and Recycling, 61*, 125–129.

Kosmatka, S. H., Kerkhoff, B., & Panarese, W. C. (2008). *Design and control of concrete mixtures* (14th ed.). Portland Cement Association.

Kosmatka, S. H., & Wilson, M. L. (2011). Design and control of concrete mixtures; EB001, 15th edition. *The guide to applications, methods, and materials* (p. 460). Portland Cement Association, Skokie, Illinois.

Majhi, R. K., & Nayak, A. N. (2019). Bond, durability and microstructural characteristics of ground granulated blast furnace slag based recycled aggregate concrete. *Construction and Building Materials, 212*, 578–595.

Neville, A. M., & Brooks, J. J. (2003). Concrete technology. *Concrete* (2nd ed., pp. 47–222). Longman Sidney, Prentice-Hall INC.

Neville, A. M., & Brooks, J. J. (2010). Concrete technology. *Concrete technology* (2nd ed., p. 402). Long man Group UK.

Newman, J., & Choo, B. S. (2003). *Advanced concrete technology*. Elsevier Ltd.

Ngugi, H. N., Mutuku, R. N., & Gariy, Z. A. (2014). Effects of sand quality on bond strength of concrete: a case study in Nairobi city county and its environs, Kenya. *International Journal of Civil and Structural Engineering Research, 2*(1), 119–129.

Prakash, S., Kumar, S., Biswas, R., & Rai, B. (2022). Influence of silica fume and ground granulated blast furnace slag on the engineering properties of ultra-high-performance concrete. *Innovative Infrastructure Solutions, 7*(117), 1–18.

Qasim, O. A., & Ahmed, A. S. (2018). Different variable effects on bond strength of normal, high and ultra-high strength concrete. *International Journal of Civil Engineering and Technology (IJCIET)., 9*, 1923–1945.

Saidi, M., Ait-Medjber, F., Safi, B., & Samar, M. (2014). Recycling of aggregates from construction demolition wastes in concrete: Study of physical and mechanical properties. *International Journal of Civil and Environmental Engineering., 8*(12), 1307–1311.

Samad, S., & Shah, A. (2017). Role of binary cement including Supplementary Cementitious Material (SCM), in production of environmentally sustainable concrete: A critical review. *International Journal of Sustainable Built Environment, 6*(2016), 663–674.

Samad, S., Shah, A., & Limbachiya, M. C. (2017). Strength development characteristics of concrete produced with blended cement using ground granulated blast furnace slag (GGBS) under various curing conditions. *Sādhanā., 42*(7), 1203–1213.

Shariq, M., Prasad, J., & Masood, A. (2013). Studies in ultrasonic pulse velocity of concrete containing GGBFS. *Construction and Building Materials, 40*, 944–950.

Singh, R. J., & Singh, R. B. (1995). Identification of expired cement by X-ray diffraction technique. *Article in Journal of the Indian Academy of Forensic Sciences, 37*, 8.

Soares, D., de Brito, J., Ferreira, J., & Pacheco, J. (2014). Use of coarse recycled aggregates from precast concrete rejects: Mechanical and durability performance. *Construction and Building Materials, 71*, 263–272.

Taffese, W. Z. (2018). Suitability investigation of recycled concrete aggregates for concrete production. *Advances in Civil Engineering, 1*, 1–11.

Yang, K. H., Jung, Y. B., Cho, M. S., & Tae, S. H. (2015). Effect of supplementary cementitious materials on reduction of CO2 emissions from concrete. *Journal of Cleaner Production., 15*(103), 774–783.
Yening, Yu., Ge, Y., & Liu, P. (2019). Recycling of expired cement and aged supplementary cementitious materials based on close packing theory and space filling effect. *Journal of Cleaner Production, 239*(118064), 11–12.
Zainudeen, N., & Jeyamathan, J. (2016). Cement and its effect to the environment: A case study in Sri Lanka. *Department of Building Economics University of Moratuwa, 1*, 1408–1416.

Publisher's Note

Springer Nature remains neutral with regard to jurisdictional claims in published maps and institutional affiliations.